The Role of the N-Terminal Heptad Repeat of HIV-1 in the Actual Lipid Mixing Step as Revealed by Its Substitution with Distant Coiled Coils†

Yael Wexler-Cohen, Kelly Sackett, and Yechiel Shai*,‡

Department of Biological Chemistry, The Weizmann Institute of Science, Rehovot 76100, Israel

Received November 2, 2004; Revised Manuscript Received January 19, 2005

ABSTRACT: The gp41 glycoprotein of HIV-1 is considered to be responsible for the actual fusion process between the virus and the host membranes. According to a prevailing model, gp41 trimer organization, directed by the N-terminal coiled-coil region (NHR), is essential for steps involved in the actual merging of viral and cellular membranes. This study addresses a major question: Is the specific sequence of the NHR obligatory for the fusion process, or can it be replaced by distant coiled coils that form different oligomeric states in solution? For this purpose we synthesized three known GCN4 coiled-coil mutants that oligomerize in solution into either dimers, trimers, or tetramers. These peptides were chemically ligated to the fusion peptide thereby creating three chimera peptides with different oligomeric tendencies in solution. These peptides were investigated, together with the 70-mer wild-type peptide (N70), regarding their structure in solution and membrane by using circular dichroism (CD) and FTIR spectroscopies, their ability to induce vesicle fusion, and their ability to bind phospholipid membranes by using surface plasmon resonance (SPR). Our results suggest that local assembly of fusion peptides, facilitated by coiled-coil oligomers, increases lipid mixing ability, probably by facilitating stronger binding of the fusion peptides to the opposing membrane as revealed by SPR. However, N70 is significantly more active than the other chimeras. Overall, the data indicate a correlation between the distinct conformation of N70 in solution and in membranes and its enhanced lipid mixing relative to the GCN4 chimeras.

The initial step in enveloped viral infection is the fusion process leading to the insertion of the virus genetic material into the host cells' cytoplasm (*1*, *2*). HIV-1, like other enveloped viruses, utilizes a specific protein embedded in its membrane to facilitate this process, termed envelope protein (ENV), and it is organized as a trimer (*3*, *4*). There are two envelope subunits associated noncovalently. The surface subunit (SU), gp120, mediates host tropism by binding specific cell receptors (reviewed in ref *5*), and the transmembrane subunit (TM), gp41, is responsible for the actual fusion event (reviewed in ref *6*). The extracellular part of gp41, the ectodomain, is composed of several regions. Specified according to their order starting from the N-terminus they include the fusion peptide (FP),[1] N-terminal heptad repeat (NHR), loop region, C-terminal heptad repeat (CHR), and the pre-transmembrane domain. The NHR is a member of a coiled-coil family subgroup; the leucine zippers (*7*, *8*). Leucine zippers have almost exclusively hydrophobic (usually leucine/isoleucine) residues in their first and fourth positions (*9*). These residues generate hydrophobic seams that facilitate oligomerization into a coiled-coil conformation (*10*).

Prior to binding of gp120 to its cellular receptors, the envelope subunits are in a metastable native conformation (*11*−*13*). At this stage gp41 is considered to be sheltered by gp120 although details concerning this conformation are essentially absent. Binding of gp120 involves major conformational changes in both glycoproteins (*14*, *15*), resulting in gp41 exposure and creation of the prehairpin conformation (*12*, *16*, *17*). In this conformation gp41 is believed to be extended, leading to the insertion of the FP into the host cell membrane, and causing its destabilization (*18*). Additional conformational changes lead to the next fusion stage: the hairpin conformation (*5*, *19*). Here, a trimeric central coiled coil is created by NHR regions exposing on its surface three conserved hydrophobic grooves into which three CHR regions pack in an antiparallel manner (*20*, *21*). Folding to hairpin conformation is presumed to induce apposition of the two membranes (*20*), and subsequent aggregation of multiple hairpin structures (*22*) presumably leads to pore formation and expansion concluding in complete fusion of the membranes (*23*).

In the predominant fusion model, described above, gp41 is considered to exist as a homotrimer throughout the fusion process (*6*, *11*, *12*), creating an oligomerized FP. Oligomerization of the FP seems to be crucial for the fusion process on the basis of several observations. In one study a mutation in the fusion peptide, V2E, had a dominant interfering effect on virus infectivity and syncytium formation (*24*). This effect was demonstrated in virus−cell and cell−cell fusion systems

† This study was supported by the Minerva Foundation.

* To whom correspondence should be addressed. Tel: 972-8-9342711. Fax: 972-9344112. E-mail: Yechiel.Shai@weizmann.ac.il.

‡ The Harold S. and Harriet B. Brady Professorial Chair in Cancer Research.

[1] Abbreviations: FP, fusion peptide; NHR, N-terminal heptad repeat; ATR-FTIR, attenuated total reflection Fourier transformed infrared; CD, circular dichroism; PC, egg phosphatidylcholine; MESNA, sodium salt of 2-mercaptoethanesulfonic acid; TFA, trifluoroacetic acid; TES, triethylsilane; RP-HPLC, reverse phase high performance liquid chromatography.

10.1021/bi047666g CCC: $30.25
Published on Web 03/25/2005

and was apparent even in the presence of excess wild-type protein, suggesting the involvement of FP oligomerization in the fusion process. A correlation between cell−cell fusion assays and model systems has been previously demonstrated utilizing the V2E construct as well as other FP mutated constructs (*25*− *27*). Additionally, an enhancement in the lipid mixing abilities of a FP oligomer versus a monomer was observed by cross-linking the fusion peptides through their C-terminus into dimers and trimers (*28*). A recent study utilized a peptide composed of the N-terminus of the FP of influenza virus attached to a trimeric C-terminal coiled coil (*29*). The influenza chimera experiments were performed in pH 7.0 and pH 5.0 and demonstrated a trimeric oligomeric state versus an aggregated state, respectively. The trimeric construct had enhanced lipid mixing ability in pH 5.0 compared to pH 7.0, but at both pHs exhibited enhanced activity compared with the monomer. This demonstrated the enhanced lipid mixing abilities of the trimer construct compared with that of the monomer.

Previous studies showed that the NHR dramatically enhances the FPs' ability to induce phospholipid membrane fusion (*30*). This combined with the fact that different viruses use different sequences in order to generate the oligomerization of their FP relates to the question: Is the specific sequence of the NHR obligatory for the fusion process, or can it be replaced by distant coiled coils that form different oligomeric states in solution? The generation of a trimeric oligomeric conformation in viral TM subunits seems to be a recurrent theme in many enveloped viruses (*31*−*34*), raising an additional question: Does trimerization match a specific role, or does it merely answer the oligomeric requirement? In order to address these questions, we analyze in this paper the influence of different oligomeric tendencies in chimera peptides mimicking the N-terminal region of gp41, on their structure and function. We synthesized three previously described (*35*) mutated GCN4 coiled coils specifying different oligomeric states in solution, namely, dimer, trimer, and tetramer. Chemical ligation between each mutant and the FP resulted in three chimera peptides with different oligomeric tendencies in solution. We investigated the peptides regarding their structure and function in comparison with the endogenous N70 (a construct composed of the FP and the gp41 NHR) generated previously (*30*), as well as the endogenous NHR. The structure of peptides in solution and membranes was determined by using circular dichroism (CD) and attenuated total reflection Fourier transform infrared (ATR-FTIR) spectroscopy, respectively. They were studied functionally for their ability to bind lipid bilayers by using surface plasmon resonance (SPR) spectroscopy, as well as their ability to induce lipid mixing of large unilamellar vesicles (LUV) composed of PC and cholesterol.

The results are discussed regarding the role of the N-terminal heptad repeat in the actual lipid mixing process and in enabling oligomerization of the fusion peptides, which markedly increases their ability to bind membranes leading to enhanced membrane destabilization and fusion.

MATERIALS AND METHODS

Materials. Boc and F-Moc amino acids, Boc MBHA resin, and F-Moc Rink Amide MBHA resin were purchased from Nova-biochem AG (Laufelfinger, Switzerland). S-Trityl-β-mercaptopropionic acid was purchased from Peptides International (Louisville, KY). Other peptide synthesis reagents, unlabeled phospholipids, cholesterol (*N*-[2-hydroxyethyl] piperazine-*N*′-[2-ethanesulfonic acid]), *N*-octyl β-D-glucopyranoside (OG), and the sodium salt of 2-mercaptoethanesulfonic acid (MESNA) were purchased from Sigma. *N*-[Lissamine rhodamine B-sulfonyl] dioleoylphosphatidylethanolamine (Rho-PE) and *N*-(7-nitrobenz-2-oxa-1,3-diazol-4-yl) dioleoylphosphatidylethanolamine (NBD-PE) were purchased from Molecular Probes (Eugene, OR). All other reagents were of analytical grade. Buffers were prepared using double-glass-distilled water. Hepes buffer is composed of 5 mM (*N*-[2-hydroxyethyl] piperazine-*N*′-[2-ethanesulfonic acid]) with 25 μM DTT to prevent creation of disulfide bonds and titrated with KOH to pH 7.2.

Peptide Synthesis. The GCN4 mutants, N36, and the FP were synthesized manually on Rink Amide MBHA resin by using the Fmoc strategy as previously described (*36*, *37*). They were cleaved from the resin using a cocktail made of TFA:DDW:TES:thioanisole:EDT (44.4:2.3:1:1:1.25 (v/v)). The "linker peptide" i.e., FP including a linker moiety (S-trityl-β-mercaptopropionic acid) which enables chemical ligation, was synthesized manually by a solid phase method on MHBA resin using BOC chemistry as described (*36*, *37*). In order to include the linker moiety, modifications outlined by Hackeng et al. (*38*) were incorporated in the protocol. The BOC peptide was cleaved from the resin by HF. All the GCN4 mutants contain a cysteine residue in their N-terminal for ligation purposes. Similarly, we replaced the N-terminal serine of N36 with cysteine to generate the wild-type N70. This position is variable in gp41, and a clone containing this residue in this specific position has been presented previously (*39*). All the peptides were purified by reverse phase high performance liquid chromatography (RP-HPLC) on a column to >98% homogeneity and lyopholized. The peptide composition and molecular weight were confirmed by platform LCA electrospray mass spectrometry and amino acid analysis.

Chemical Ligation. The following modifications were added to the previously described ligation protocol (*38*): (1) MESNA was used as the catalyst (*40*). (2) The pH of the reaction mixture made of 6.0 M guanidine hydrochloride (GuHCL), 0.1 M Na_2HPO_4 and 1% (w/v) MESNA was adjusted to ∼7.2 using 1 M NaHO. (3) The range of peptides concentrations in the ligations was 0.2 mM to 1.9 mM. (4) The various ligations were incubated for 2−3 days at room temperatures and then transferred to 4 °C for a period of 2−3 weeks. The wt, N70, ligation was performed separately as previously described, with the exception of the location of the cysteine residue in N70 and the lengths of the two unjoined peptides (*30*). Each ligation product was purified by RP-HPLC to >98% homogeneity. Their composition and molecular weight were confirmed by electrospray mass spectroscopy and amino acid analysis.

Circular Dichroism (CD) Spectroscopy. CD measurements were performed on an Aviv 202 spectropolarimeter. The spectra were scanned using a thermostatic quartz cuvette with a path length of 1 mm at 25 °C. The average time recording of each spectra was 20s in 1 nm steps in the wavelength range of 190−260 nm. The peptides were scanned at a concentration of 10 μM in HEPES buffer.

ATR-FTIR Spectroscopy. Spectra were obtained with a Bruker equinox 55 FTIR spectrometer equipped with a deuterated triglyceride sulfate (DTGS) detector and coupled with an ATR device. One hundred fifty scans were collected for each spectrum with 4 cm^{-1} resolution at room temperature. Prior to sample preparation the peptides were dissolved in 0.1 M HCL and lyophilized several times in order to replace the trifluoroacetate (CF_3COO^-) counterions with chloride ions. Peptides were dissolved in MeOH and lipids in a 2:1 $CHCL_3$/MeOH mixture. Samples were prepared as described (*41*) and spread on a ZnSe ATR prism (80 mm/7 mm). The lipid−peptide molar ratio of the samples was 1:400. After the samples were applied, the prism was placed under vacuum for 30 min in order to dry the solvents. The samples were hydrated by incubating for 6 min with an excess of deuterium oxide before acquisition of the data. Pure deuterated phospholipid spectra were subtracted to yield the difference spectra (*25*, *41*−*43*).

ATR-FTIR Data Analysis. We analyzed the data using PEAKFIT (Jandel Scientidic, San Rafael, CA) software. The positions of the component peaks were calculated using the second derivative spectra. These wavenumbers were used as the initial parameters for curve fitting with Gaussian component peaks. Positions, bandwidths, and amplitudes of the peaks were varied until a good agreement between the calculated sum of all components and the experimental spectra was achieved ($r^2 > 0.997$) under the following constraints: (1) the resulting bands shifted by no more than 2 cm^{-1} from the initial second derivative assignment and (2) all the peaks had reasonable half-widths ($<20-25$ cm^{-1}). Dividing an individual peak area assigned to a particular secondary structure by the whole absorbance area of the amide band gave the relative amount of that particular secondary structure (*44*).

Preparation of Large (LUV) and Small Unilamellar Vesicles (SUV). Thin films of PC and cholesterol mixture at a molar ratio of 9:1, respectively, were generated following dissolution of the lipids in a 2:1 (v/v) mixture of $CHCL_3$/MeOH and then dried under a stream of nitrogen gas while rotating. Two populations of films were generated: (1) PC:Chol mixture as described above termed "unlabeled" and (2) the same lipid mixture containing 0.6% molar of NBD-PE and RHO-PE each, termed "labeled". The films were lyopholized overnight, sealed with argon gas to prevent oxidation of the lipids, and stored at −20 °C. Before the experiment, the films were suspended in the appropriate buffer and vortexed for 1.5 min. The lipid suspension underwent five cycles of freezing−thawing and then extrusion through polycarbonate membranes with 1 μm and 0.2 μm diameter pores for 21 times to create the large unilamellar vesicles. In order to prepare the small unilamellar vesicles, PC:Chol (9:1 w/w) films were dissolved in the appropriate buffer, vortexed for 1.5 min, sonicated as previously described for production of SUVs (*45*), and diluted to 0.5 mM in the appropriate buffer.

Peptide Induced Lipid Mixing. All fluorescence measurements were performed on a SLM-AMINCO Bowman series 2-luminescence spectrometer at 25 °C, and the lipid mixing of the LUV was measured using a fluorescence-probe dilution assay (*46*). LUVs were prepared with HEPES buffer as described above from unlabeled and labeled films and combined together to create a 9:1 mixture of unlabeled to labeled vesicles in 110 μM total lipid concentration. The fluorescence level was measured initially with the vesicle mixture alone and then following the addition of a peptide dissolved in a small volume of dimethyl sulfoxide (DMSO with 5 mM DTT). All measurements were performed in a quartz cuvette with constant magnetic stirring. Peptides' concentrations were calculated either as monomers or per oligomer while taking into account the specific oligomeric state. Maximal increase in fluorescence was observed 1−2 min after addition of the peptide, similarly to what has been observed by others with covalently linked HIV-1 fusion peptide (*28*). Data was collected for several additional minutes to ensure a steady state indicated by a plateau. In addition, in all cases measurements began about 1 min after addition of the peptide, and therefore measurements for all peptides were recorded under the same time scale. The increase in NBD fluorescence, the energy donor, at 530 nm was monitored with the excitation set at 467 nm. The fluorescence intensity before the peptide addition was referred to as 0% lipid mixing. The fluorescence intensity after addition of reduced Triton xs-100 (0.05% (v/v)) was referred to as 100% lipid mixing.

Binding Analysis by SPR Biosensor. Biosensor experiments were carried out with a BIAcore X analytical system 3000 (BIAcore, Uppsala, Sweden) using an L1 sensor chip (BIAcore) at 25 °C. The chip contains hydrophobic aliphatic chains that include exposed polar headgroups. When the SUVs are applied to the chip surface, they interact with the polar headgroups, resulting in a bilayer lipid surface formation. The protocol used for the binding experiments was previously described (*47*, *48*) with several alterations: (1) Peptide solutions were 1.25 μM for the HIV-GCN4 chimera and N70 peptides. (2) Peptide solutions of 50−100 μL were injected each time at 5 μL/min flow rate. (3) The running buffer and the buffer used to dissolve the peptides was HEPES buffer. The dissociation was performed with only the running buffer, and the time corresponded to the specific peptide and its concentration. SPR detects changes in the refractive index of the surface layer of peptides and lipids in contact with the sensor chip. Sensograms were obtained by plotting the response units against time.

Determining Peptides Oligomeric State by SDS−PAGE. HIV-GCN4 chimera and N70 peptides were dissolved in sample buffer composed of 2% (w/v) SDS, 0.0025 M β-mercapthoethanol, 0.065 M TRIS-HCL (pH 6.8), and 10% (v/v) glycerol. The samples were then sonicated and loaded on an SDS−PAGE gel with 16% SDS in the separating gel fraction. The gels were stained with 1% Coomassie blue dissolved in a fixer solution composed of 25% isopropanol and 7% glacial acetic acid in ddH_2O.

RESULTS

We produced three chimera peptides comprising mutated forms of the GCN4 leucine zipper fused to the FP of HIV-1, as well as the wt N70 composed of the FP and the NHR regions. The final products following peptide synthesis, various ligations, purification, and verification of their amino acid content are presented in Figure 1. The GCN4 mutants were chosen for this study on the basis of the small size of their oligomerization determining region (enabling the substitution of the NHR by them), their ability to create

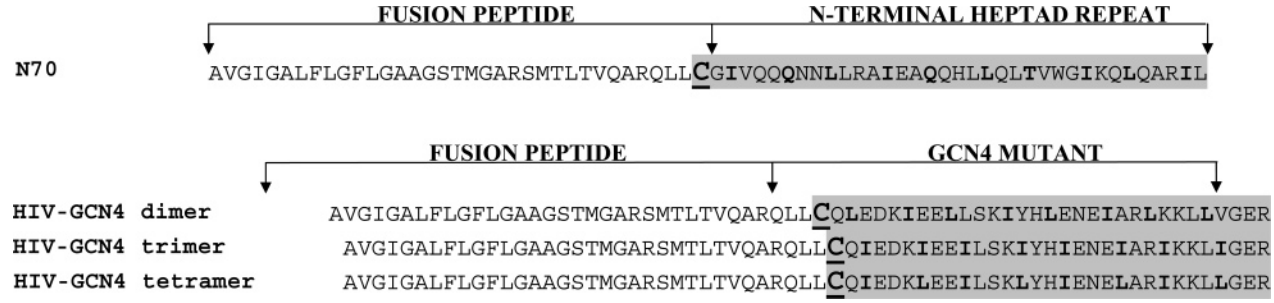

FIGURE 1: Schematic representation of the peptides utilized in this paper. The wt sequence (N70), gp41 N-terminal segment, including the FP and the NHR is presented at the top, with the N36 region highlighted (heptad repeat positions a and d in bold). We chose a site for ligation at the border of the NHR which is variable, and is wild type in the primary isolate CA5 (*39*). Sequences of the various chimeras designed for the study are presented at the bottom; each contains the FP fragment ligated chemically to a different GCN4 mutant (highlighted). The residues responsible for the variations (heptad repeat positions a and d) are in bold. The cysteine residue enabling the ligation for N70 and the chimeras is underlined.

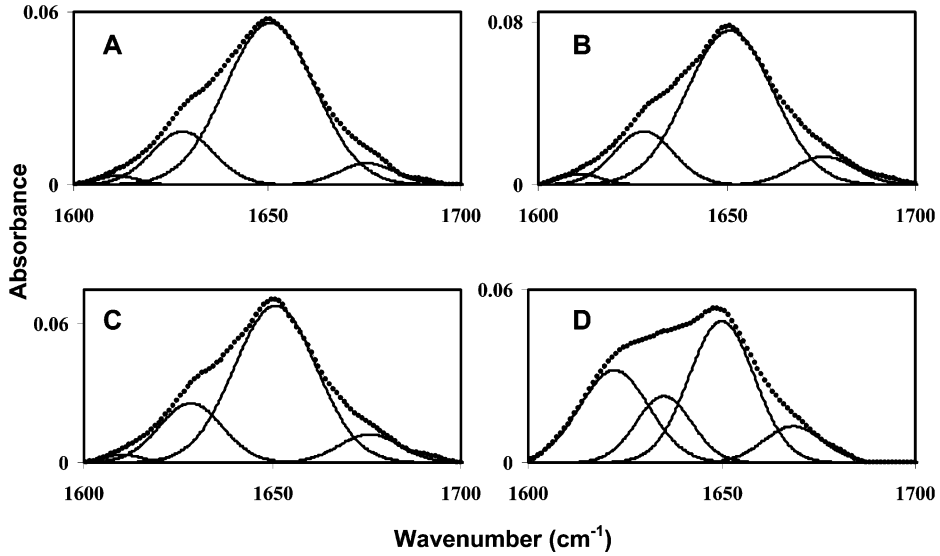

FIGURE 2: ATR−FTIR spectra deconvolution of the fully deuterated amide 1 band. Peptides HIV-GCN4 dimer, HIV-GCN4 trimer, HIV-GCN4 tetramer, and N70 are represented by A, B, C, and D, respectively. The dotted line represents the sum of the individual fitted components. The fitted spectrum superimposes the experimental spectrum collected after Savitzky-Golay smoothing with good agreement ($R^2 = 0.99$). The individual fitted components are represented by a continuous line below.

parallel oligomers, and their specified oligomerization abilities. The continuity of the heptad repeat first and fourth positions was preserved in the design of the chimera peptides (see Figure 1).

Peptides' Structure in the Membrane Determined by Using ATR-FTIR Spectroscopy. The secondary structure of the peptides was determined following their incorporation into PC:Chol multilayers. This was done to check whether the attachment of the different coiled coils to the fusion peptide had an effect on its reported β-sheet structure (*49*). The different component peaks, created following curve fitting, for the three HIV-GCN4 chimeras as well as for N70 are shown in Figure 2. Their assignments and relative areas are specified in Table 1. The results reveal that the different chimeras are almost identical regarding their secondary structure composition. Their α-helical content is 74%, 71%, and 69% while their β-sheet content is 23%, 26%, and 29% for the HIV-GCN4 dimer, trimer, and tetramer, respectively. The N70 results, with 53% helical content and 47% β content (divided into β-sheet and β-sheet aggregates), correspond to data obtained previously (*49*). This is in agreement with the notion that the 16 N-terminal amino acids of HIV-1 gp41 adopt a β-sheet structure in the membrane. We interpret these findings as a structural interplay between heptad repeat and FP regions meaning that there might be certain structural flexibility at the seam of the heptad repeat and the FP, depending on the secondary structure tendencies of flanking sequences. Possibly the GCN4 moiety in the GCN4 chimeras induces an extension of the coiled coil toward the FP while in the N70 the NHR is a weaker α-helical inducer, therefore,

Table 1: Secondary Structure Content Specified by ATR-FTIR Spectroscopy[a]

peptide	α-helix ~1650−1654 cm^{-1}	β-sheet ~1625−1640 cm^{-1}	β-turn ~1670−1685 cm^{-1}	other
HIV-GCN4				
dimer	1651 (74.8%)	1628 (16.8%)	1676 (6.6%)	1611 (1.7%)
trimer	1651 (71.6%)	1628 (16.9%)	1676 (9.1%)	1611 (2.2%)
tetramer	1651 (69.3%)	1628 (20%)	1676 (9.1%)	1610 (1.5%)
N70	1650 (43.3%)	1635 (17.1%)		1622.2 (29.6%)[b] 1668.5 (9.9%)[c]

[a] Each component peak wavenumber in the spectral deconvolution is indicated. In parentheses the percent area relative to the component contribution is specified. The characteristic amide 1 frequencies of the various secondary structures were taken from Jackson and Mantsch (*44*). [b] Represents β-sheet aggregates (1620−1625 cm^{-1}). [c] Represents 3_{10} helix (1655−1670 cm^{-1}).

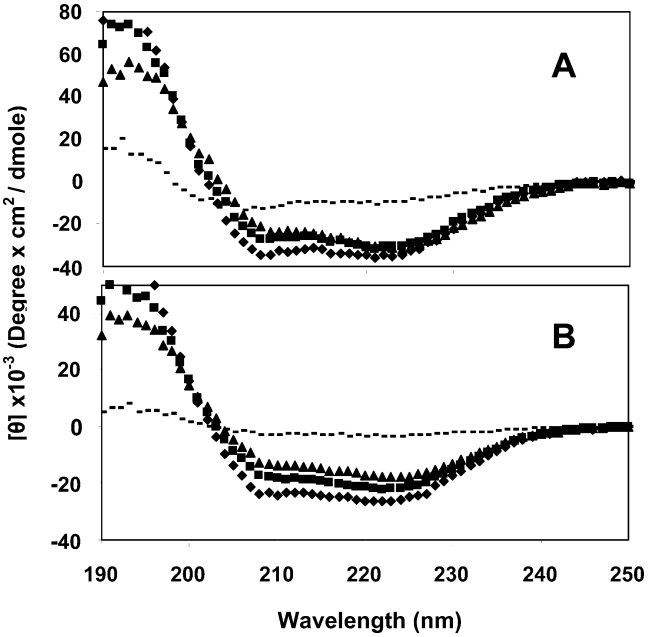

FIGURE 3: CD spectra of 10 μM heptad repeat peptides (panel 3A) and the chimeras (panel 3B) in HEPES buffer. GCN4 (and the corresponding chimeras) dimer, trimer, and tetramer are represented by filled diamonds, triangles, and squares, respectively, while the N36 (and the corresponding N70 chimera) is represented by a broken line.

the β-sheet of the FP induces an extension of a β structure toward the NHR.

Oligomer Formation Determined by Using CD Spectroscopy. CD spectroscopy was utilized in order to test whether the different GCN4 peptides create oligomers in solution. The data (Figure 3A) clearly demonstrate that the three GCN4 mutants have a distinct α-helical structure with minima at 222 nm and 208 nm. Previous studies have shown that the ratio of the ellipticities at 222 nm and 208 nm can be utilized to distinguish between the monomeric and oligomeric states of a coiled coil (*50*−*52*). When the ratio $\theta_{222}/\theta_{208}$ equals about 0.8, the coiled-coil protein is in its monomeric state, and when the ratio exceeds the value of 1.0, the coiled-coil protein is in its oligomeric state. The data reveal values of 1.01, 1.12, and 1.46 for the GCN4 dimer, trimer, and tetramer, respectively, all of which exceed 1.0. This supports the notion that the GCN4 mutants are present in oligomeric states as was already demonstrated (*35*). For the equivalent endogenous peptide, the NHR, the situation is different. Although it has the general α-helix profile, the signal is reduced significantly compared with the GCN4 mutants. This implies that the NHR has either a reduced α-helical content by itself or a less stable α-helix moiety in a solution environment. We also measured the CD spectra of all the chimeras in buffer, and the spectra are shown in Figure 3B. The CD spectra of the chimera constructs were taken under the same pH condition used for the GCN4 mutated peptides shown in Figure 3A, which have been previously shown to create dimers, trimers, and tetramers in solution (*35*). The data reveal that the CD spectra of the chimera proteins are almost identical to those of the corresponding GCN4 peptides. Note, however, that the overall elipticities of the chimeras are lower than those of the GCN4 peptides since the additional 34 amino acids may only partially contribute to the α-helical structure in solution. In addition, the FP alone does not aggregate under the same conditions (see the following section); therefore we can assume that a significant fraction of the chimeras exist in the same oligomeric state as the mutated GCN4 peptides. In support of this, when the FP of influenza was attached to a discrete trimeric coiled coil, it formed a trimer at pH 7 (*29*), although when the pH was reduced to 5.0, higher oligomers were detected. Nevertheless, we cannot rule out the possibility that there are some differences between the GCN4 parental peptides and the chimeras.

The Oligomeric State of the 33-mer Fusion Peptide Determined by Using Rho Fluorescence Measurements. The tendency of the fusion peptide to self-associate in solution was tested using a Rho-labeled peptide. Since Rhodamine fluorescence intensity is highly sensitive to self-quenching, changes in the fluorescence intensity of Rho-labeled peptide may be attributed mainly to changes in its oligomeric state. If the Rho-labeled peptide forms homooligomers, its fluorescence is quenched. When Proteinase K is added, the peptides are cleaved into small peptidic fragments. As a consequence, oligomers, if there are any, dissociate, causing an increase in the fluorescence intensity. Thus, the final Rhodamine fluorescence intensity can be considered as that of a monomeric Rho-labeled peptide. Briefly, Proteinase K (10 mg/mL) was added to 1 μM Rho-labeled peptide in 5 mM HEPES buffer containing 25 μM DTT. Fluorescence intensity at 580 nm (4 nm slit) was recorded as a function of time before and after the addition of the enzyme and found to be the same. Excitation was set at 530 nm (4 nm slit). These data demonstrate that the 33-mer fusion peptide is not aggregated in solution. A similar assay revealed that the internal fusion peptides of Sendai and measles viruses are oligomers in solution (*53*, *54*).

Peptides' Induced Lipid Mixing. All peptides were tested regarding their ability to induce lipid mixing of LUV composed of PC/chol. The results are presented in Figure 4. The FP alone (a 33-mer peptide) used as a control has the lowest lipid mixing ability. Similar results were obtained if the peptides were first equilibrated in buffer and then added to vesicles, or the peptides were added directly from a DMSO solution, suggesting that the peptides first equilibrate in buffer and then bind to vesicles. The data reveal a marginal difference between the results calculated on the basis of the monomeric or the oligomeric states of all the GCN4 constructs. However, under the same conditions the N70 shows a markedly higher lipid mixing ability. The kinetics for all the peptides was very fast, and measurements in all cases were made at equilibrium within 1−2 min after addition of the peptide. Since the GCN4's by themselves showed no lipid mixing abilities (data not shown), these results reveal that (i) the fusion peptide preserves its fusogenic activity even though it was attached to a piece of unrelated protein; (ii) replacing the NHR with another unrelated coiled coil slightly increases the lipid mixing ability of the fusion peptide apparently independent of the oligomeric state of the coiled coil in solution, although we cannot preclude the possibility that in each case the monomer or the dimer form of the chimera peptides was responsible for the lipid mixing action due to the dissociation of the coiled coils in the membrane (see comments in the SDS experiments); and (iii) the N70 has enhanced lipid mixing ability which implicates the specific sequence of the NHR as a direct

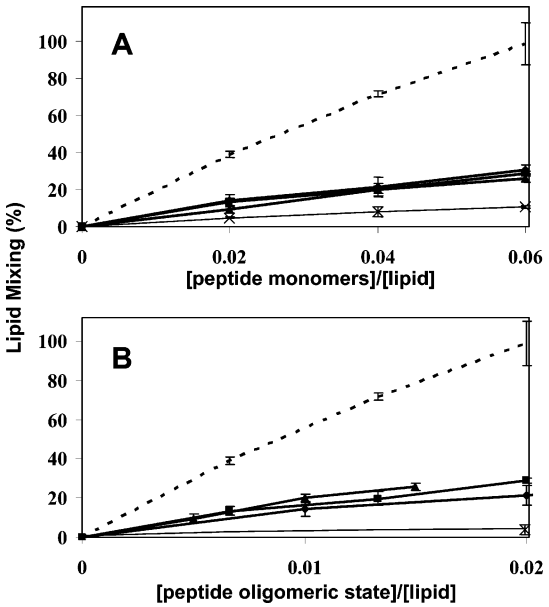

FIGURE 4: Lipid mixing results of PC/Chol LUV induced by the peptides. For each point of experimental measurement, the standard deviation is bracketed. Panel A presents the results based on the concentration of monomers creating oligomers, and panel B presents the experimental results adjusted according to the concentration of the number of oligomers for each peptide. Peptide designations are as follows: HIV N70, broken line; HIV-GCN4 dimer, filled diamonds; trimer, filled squares; tetramer, filled triangles; 33-mer FP, crosses.

contributor to the lipid mixing potential of the FP, alongside its role to induce oligomerization of fusion peptides in order to enhance their fusion ability.

Binding of the Peptides to PC/Chol Membranes Determined by Using SPR Biosensor. The potencies of the different peptides to induce lipid mixing were tested under similar peptide:lipid molar ratios. Under these conditions the three chimeras had similar activities. However, this would suggest that they have similar membrane perturbing capacities only if their affinities to the membranes are also similar. To address this issue we performed a binding assay with the chimeras, as well as N70 by using BIAcore biosensor. The peptides at 1.25 μM were allowed to interact with PC/Chol bilayers on the surface of a LI chip. The corresponding sensograms were constructed. All three HIV-GCN4 chimera peptides showed practically irreversible binding. Figure 5 presents the sensogram of HIV-GCN4 trimer as the chimeras' representative as well as N70. These results demonstrate that all the chimera peptides bind irreversibly to PC/Chol membranes at the concentrations present in the lipid mixing assay and therefore support our assumption that all the chimeras have a similar potency in inducing membrane fusion. In contrast with the chimera peptides, the N70 does not bind the PC/Chol membrane irreversibly at the indicated concentration and dissociates. This supports the conclusion that, although not quantitatively evaluated, the potency of N70 in inducing membrane fusion in comparison with the chimeras is even greater than that observed in the lipid mixing assay (Figure 4).

The Oligomeric State of the Peptides within SDS−PAGE. SDS−PAGE gel which can partially mimic negatively charged membranes was used to estimate the oligomeric state of the different chimera peptides in a membrane-like environment (Figure 6). We cannot rule out the possibility

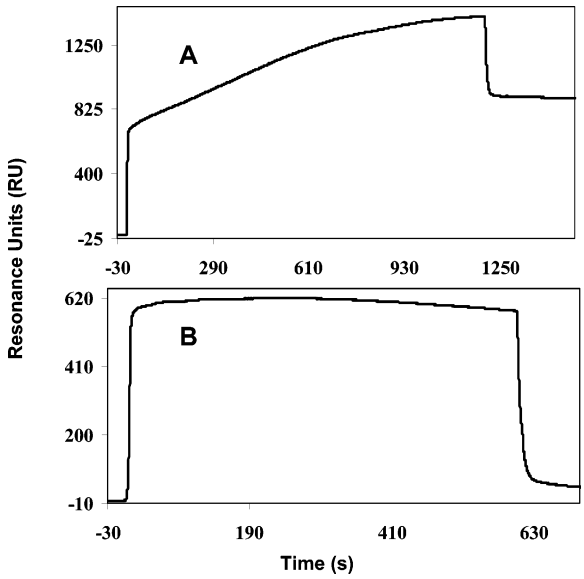

FIGURE 5: The binding sensograms between peptides and the PC:Chol (9:1 w/w) lipid bilayer: (A) HIV-GCN4 trimer at 1.25 μM and (B) N70 1.25 μM.

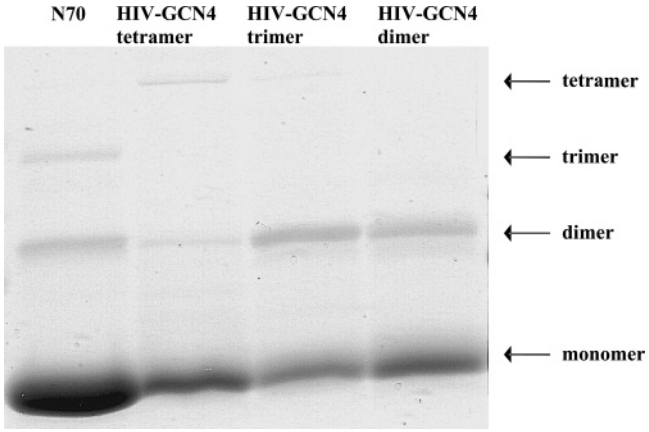

FIGURE 6: Determination of the chimeras' oligomeric state by SDS−PAGE. The expected molecular weight for the dimer, trimer, and tetramer chimera oligomeric states is 14174, 21261, and 28348 g/mol, respectively. For the wt, N70, the dimer and trimer oligomeric states are 14916 and 22374 g/mol, respectively. Higher amounts of HIV-GCN4 chimera peptides did not change the observed pattern.

that SDS drives the dissociation of the oligomers. Indeed we have shown previously that the HIV-1 NHR dissociates in negatively charged membranes (*55*) but with slow kinetics. Furthermore, previous studies have also shown that the GCN4 coiled coils tend to dissociate into their monomeric state in the presence of SDS (*50*). This might influence the oligomerization ability of all the chimeras in the SDS gel and shift the equilibrium toward the monomeric form. In this study the peptides reach the membrane from a solution mainly as oligomers (as discussed previously) and the kinetics of the fusion event is very fast (∼1−2 min) (figure not shown). We therefore can assume that the initial fusion-active form has a high fraction of oligomeric structure. The SDS gel shows that, even after a long time of incubation with this detergent, the different constructs retain characteristic oligomeric profiles. We could not obtain a trimer oligomeric form of the HIV-GCN4 trimer mutant in SDS, an observation already made earlier for the GCN4 trimer mutant in a previous study (*56*), but rather an intermediate

form between the HIV-GCN4 dimer and the HIV-GCN4 tetramer. Nevertheless, all the constructs showed different profiles, thus demonstrating that the different heptad repeats have different oligomeric properties. Note that higher amounts of HIV-GCN4 chimera peptides did not change the observed pattern in Figure 6.

DISCUSSION

In this study we substituted the N-terminal heptad repeat of the HIV-1 N70 peptide with other known unrelated heptad repeats, creating FP chimera constructs with different oligomeric tendencies in solution: a dimer, trimer, and a tetramer. The structures of the chimeras in PC/Chol membranes were determined by using ATR-FTIR spectroscopy and revealed a strong helical component for all the HIV-GCN4 chimera peptides, as expected, and a smaller β component compared with the wild-type N70. It seems as though there is a delicate balance between the two secondary structure elements that depends on the secondary structure tendency of the coiled coil and the FP. The GCN4 mutants have very strong α-helical propensity, and therefore they can induce an extension of the α-helix structure toward the C-terminal region of the FP in the chimeras. In N70, apparently, the NHR is a weaker α-helix inducer compared with the GCN4 moieties; therefore the FP probably induces an extension of the β-sheet structure toward it. This hypothetical requirement might be explained by the differences in the sequence nature of the NHR compared with the mutated GCN4 peptides. Both belong to the Leucine zipper family, but the NHR includes a substantial amount of nonhydrophobic amino acids in its first and fourth heptad positions (three are not leucine/isoleucine but polar residues out of 10 residues while in the GCN4 mutants all eight are only leucine/isoleucine).

The CD experiments were performed in order to confirm that the GCN4 mutants as well as the chimera peptides do create oligomers in solution. We used GCN4 mutants with a well-defined oligomeric state in solution, previously shown to create dimers, trimers, and tetramers (*35*). The formation of oligomeric helices is also demonstrated by their $\theta_{222}/\theta_{208}$ ratio (*50*−*52*). Since the shape of the chimera CD spectra is almost identical to that of the GCN4 peptides (Figure 3), we assume that the chimeras exist in the same oligomeric state as the mutated GCN4 peptides in solution. Further support for this is the finding that a chimera composed of the FP of influenza and a discrete trimeric coiled coil formed a trimer at pH 7 (*29*). We therefore believe that, although heterogeneous oligomeric states are probably present in solution, the main oligomeric species of the chimera peptides is dictated by the GCN4 mutated moiety.

The lipid mixing assay revealed that, in contrast to the HIV-GCN4 chimera constructs, N70 showed a higher lipid mixing ability under the same conditions (Figure 4). This result implies that the specific NHR sequence is essential for an increased efficiency in the lipid mixing event. This observation strengthens previous studies in which it was demonstrated that the N70 construct had dramatically enhanced ability to induce phospholipid membrane fusion compared with the FP alone (*30*, *57*). Note that the differences in the activities of the GCN4 chimeras based either on their monomer concentration (Figure 4A) or oligomer concentration (Figure 4B) are significantly lower compared with the difference between them and N70. On the basis of the above, it appears that a specific oligomeric tendency is not obligatory for enhanced lipid mixing ability although we cannot preclude the possibility that in some cases the same oligomeric form is responsible for the lipid mixing.

As discussed in details in the section on the oligmeric state of the chimeras in SDS, we cannot rule out the possibility that this detergent (which partially mimics acidic membrane environment) slowly drives the dissociation of the chimeras, similarly to what has been shown with HIV-1-NHR in negatively charged membranes (*55*). Another support for this possibility is the finding that the GCN4 coiled coils tend to dissociate to monomers in the presence of SDS (*50*). However, since the peptides reach the membrane from a solution as mainly oligomers (as discussed previously) and the kinetics of the fusion event is very fast (∼1−2 min) (figure not shown), we assume that the chimera's oligomers are the initial fusion-active forms. Overall, the oligomeric states shown here in the SDS gel (Figure 6) should not be considered as the actual fusogenic species but rather show that, even after a long time of incubation with this detergent, there are still some fractions of oligomers, which vary among the different constructs, although similar patterns were observed for the dimer and trimer.

The membrane binding assay for the HIV-GCN4 peptides revealed irreversible binding at the concentrations used in the lipid mixing assay. This supports the notion that the chimera peptides are similar in their lipid mixing potencies. In contrast, the N70 peptide binds phospholipids reversibly. Combined with the lipid mixing results this indicates a higher potency for lipid mixing abilities compared with the HIV-GCN4 chimera peptides.

A correlation exists between the different structures obtained for the chimera peptides versus the N70 peptide and their lipid mixing abilities, which may explain the enhanced ability of the N70 in lipid mixing. The N70 construct has a higher β-sheet content and a lower α-helical content compared with the HIV-GCN4 chimera peptides in phospholipid membranes. The additional β-sheet content of the N70 possibly enables better membrane destabilization by the FP through improved oligomerization.

The NHR region itself seems to be crucial for the fusion event in three intertwined aspects. The first is structural, enabling the creation of the hairpin conformation initiated by NHR trimeric coiled-coil formation. The second seems to be an ability to increase the lipid mixing ability of the FP by other means than oligomerization, based on the present findings. This ability is probably based on the NHR specific sequence and is strengthened by the fact that different viruses that use the same fusion mechanism utilize different heptad sequences and no "consensus/homologous" sequence exists (*31*−*34*, *58*, *59*). The third possible role for the NHR region is to enable the oligomerization of the FP in order to enhance local destabilization and fusion. This is based on several observations: (i) the NHR addition to the FP enhances the FP ability to induce lipid mixing (*30*), (ii) an enhanced fusogenic ability of fusion peptides upon their oligomerization (*28*, *29*), and (iii) the NHR induces oligomerization of otherwise monomeric proteins fused to its N-terminus (*60*, *61*).

The question of "why a trimer?" remains. Possibly the advantage of a trimer depends on the context of the whole gp41 polypeptide. For example, it is possible that trimerization enables the utilization of a minimal number of monomers needed for creation of a coiled coil with appropriate grooves in order to facilitate the hairpin formation and creation of localized oligomerized fusion peptides thereby saving energy. Another explanation could be that trimerization has a structural or energetic role preceding the actual fusion event, for example in the metastable or prehairpin conformations or even during gp160 synthesis, processing, and transport.

In summary, this study strengthens the notion that there are additional roles for the NHR region of the HIV-1 gp41 besides the structural participation in the hairpin conformation, namely, enhancing lipid mixing and fusion abilities by both oligomerization of fusion peptides and yet an unknown mechanism dictated by the NHR specific sequence.

REFERENCES

1. White, J. M. (1992) Membrane fusion, *Science 258*, 917−924.
2. Chernomordik, L. V., and Kozlov, M. M. (2003) Protein-lipid interplay in fusion and fission of biological membranes *Annu. Rev. Biochem. 72*, 175−207.
3. Zhang, C. W., Chishti, Y., Hussey, R. E., and Reinherz, E. L. (2001) Expression, purification, and characterization of recombinant HIV gp140. The gp41 ectodomain of HIV or simian immunodeficiency virus is sufficient to maintain the retroviral envelope glycoprotein as a trimer, *J. Biol. Chem. 276*, 39577−39585.
4. Center, R. J., Leapman, R. D., Lebowitz, J., Arthur, L. O., Earl, P. L., and Moss, B. (2002) Oligomeric structure of the human immunodeficiency virus type 1 envelope protein on the virion surface, *J. Virol. 76*, 7863−7867.
5. Clapham, P. R., and McKnight, A. (2002) Cell surface receptors, virus entry and tropism of primate lentiviruses, *J. Gen. Virol. 83*, 1809−1829.
6. Chan, D. C., and Kim, P. S. (1998) HIV entry and its inhibition, *Cell 93*, 681−684.
7. Delwart, E. L., Mosialos, G., and Gilmore, T. (1990) Retroviral envelope glycoproteins contain a "leucine zipper"-like repeat, *AIDS Res. Hum. Retroviruses 6*, 703−706.
8. Wild, C., Dubay, J. W., Greenwell, T., Baird, T., Jr., Oas, T. G., McDanal, C., Hunter, E., and Matthews, T. (1994) Propensity for a leucine zipper-like domain of human immunodeficiency virus type 1 gp41 to form oligomers correlates with a role in virus-induced fusion rather than assembly of the glycoprotein complex, *Proc. Natl. Acad. Sci. U.S.A. 91*, 12676−12680.
9. Landschulz, W. H., Johnson, P. F., and McKnight, S. L. (1988) The leucine zipper: a hypothetical structure common to a new class of DNA binding proteins, *Science 240*, 1759−1764.
10. Cohen, C., and Parry, D. A. D. (1986) α-Helical coiled coils—a widespread motif in proteins, *TIBS 11*, 245−248.
11. Weissenhorn, W., Dessen, A., Calder, L. J., Harrison, S. C., Skehel, J. J., and Wiley, D. C. (1999) Structural basis for membrane fusion by enveloped viruses, *Mol. Membr. Biol. 16*, 3−9.
12. Eckert, D. M., and Kim, P. S. (2001) Mechanisms of viral membrane fusion and its inhibition, *Annu. Rev. Biochem. 70*, 777−810.
13. Dimitrov, A. S., Xiao, X., Dimitrov, D. S., and Blumenthal, R. (2001) Early intermediates in HIV-1 envelope glycoprotein-mediated fusion triggered by CD4 and co-receptor complexes, *J. Biol. Chem. 276*, 30335−30341.
14. Jones, P. L., Korte, T., and Blumenthal, R. (1998) Conformational changes in cell surface HIV-1 envelope glycoproteins are triggered by cooperation between cell surface CD4 and co-receptors, *J. Biol. Chem. 273*, 404−409.
15. Poranen, M. M., Daugelavicius, R., and Bamford, D. H. (2002) Common principles in viral entry, *Annu. Rev. Microbiol. 56*, 521−538.
16. Furuta, R. A., Wild, C. T., Weng, Y., and Weiss, C. D. (1998) Capture of an early fusion-active conformation of HIV-1 gp41, *Nat. Struct. Biol. 5*, 276−279.
17. Melikyan, G. B., Markosyan, R. M., Hemmati, H., Delmedico, M. K., Lambert, D. M., and Cohen, F. S. (2000) Evidence that the transition of HIV-1 gp41 into a six-helix bundle, not the bundle configuration, induces membrane fusion, *J. Cell. Biol. 151*, 413−423.
18. Durell, S. R., Martin, I., Ruysschaert, J. M., Shai, Y., and Blumenthal, R. (1997) What studies of fusion peptides tell us about viral envelope glycoprotein-mediated membrane fusion (review), *Mol. Membr. Biol. 14*, 97−112.
19. Colman, P. M., and Lawrence, M. C. (2003) The structural biology of type I viral membrane fusion, *Nat. Rev. Mol. Cell. Biol. 4*, 309−319.
20. Weissenhorn, W., Dessen, A., Harrison, S. C., Skehel, J. J., and Wiley, D. C. (1997) Atomic structure of the ectodomain from HIV-1 gp41, *Nature 387*, 426−430.
21. Chan, D. C., Fass, D., Berger, J. M., and Kim, P. S. (1997) Core structure of gp41 from the HIV envelope glycoprotein, *Cell 89*, 263−273.
22. Munoz-Barroso, I., Durell, S., Sakaguchi, K., Appella, E., and Blumenthal, R. (1998) Dilation of the human immunodeficiency virus-1 envelope glycoprotein fusion pore revealed by the inhibitory action of a synthetic peptide from gp41, *J. Cell. Biol. 140*, 315−323.
23. Markosyan, R. M., Cohen, F. S., and Melikyan, G. B. (2003) HIV-1 Envelope Proteins Complete Their Folding into Six-helix Bundles Immediately after Fusion Pore Formation, *Mol. Biol. Cell. 14*, 926−938.
24. Freed, E. O., Delwart, E. L., Buchschacher, G. L., Jr., and Panganiban, A. T. (1992) A mutation in the human immunodeficiency virus type 1 transmembrane glycoprotein gp41 dominantly interferes with fusion and infectivity, *Proc. Natl. Acad. Sci. U.S.A. 89*, 70−74.
25. Pritsker, M., Rucker, J., Hoffman, T. L., Doms, R. W., and Shai, Y. (1999) Effect of nonpolar substitutions of the conserved Phe11 in the fusion peptide of HIV-1 gp41 on its function, structure, and organization in membranes, *Biochemistry 38*, 11359−11371.
26. Kliger, Y., Aharoni, A., Rapaport, D., Jones, P., Blumenthal, R., and Shai, Y. (1997) Fusion peptides derived from the HIV type 1 glycoprotein 41 associate within phospholipid membranes and inhibit cell-cell Fusion. Structure-function study, *J. Biol. Chem. 272*, 13496−13505.
27. Pereira, F. B., Goni, F. M., and Nieva, J. L. (1995) Liposome destabilization induced by the HIV-1 fusion peptide effect of a single amino acid substitution, *FEBS Lett. 362*, 243−246.
28. Yang, R., Yang, J., and Weliky, D. P. (2003) Synthesis, enhanced fusogenicity, and solid state NMR measurements of cross-linked HIV-1 fusion peptides, *Biochemistry 42*, 3527−3535.
29. Lau, W. L., Ege, D. S., Lear, J. D., Hammer, D. A., and DeGrado, W. F. (2004) Oligomerization of fusogenic peptides promotes membrane fusion by enhancing membrane destabilization, *Biophys. J. 86*, 272−284.
30. Sackett, K., and Shai, Y. (2002) The HIV-1 gp41 N-terminal heptad repeat plays an essential role in membrane fusion, *Biochemistry 41*, 4678−4685.
31. Kobe, B., Center, R. J., Kemp, B. E., and Poumbourios, P. (1999) Crystal structure of human T cell leukemia virus type 1 gp21 ectodomain crystallized as a maltose-binding protein chimera reveals structural evolution of retroviral transmembrane proteins, *Proc. Natl. Acad. Sci. U.S.A. 96*, 4319−4324.
32. Malashkevich, V. N., Singh, M., and Kim, P. S. (2001) The trimer-of-hairpins motif in membrane fusion: Visna virus, *Proc. Natl. Acad. Sci. U.S.A. 98*, 8502−8506.
33. Zhao, X., Singh, M., Malashkevich, V. N., and Kim, P. S. (2000) Structural characterization of the human respiratory syncytial virus fusion protein core, *Proc. Natl. Acad. Sci. U.S.A. 97*, 14172−14177.
34. Weissenhorn, W., Carfi, A., Lee, K. H., Skehel, J. J., and Wiley, D. C. (1998) Crystal structure of the Ebola virus membrane fusion subunit, GP2, from the envelope glycoprotein ectodomain, *Mol. Cell 2*, 605−616.
35. Harbury, P. B., Zhang, T., Kim, P. S., and Alber, T. (1993) A switch between two-, three-, and four-stranded coiled coils in GCN4 leucine zipper mutants, *Science 262*, 1401−1407.
36. Merrifield, R. B., Vizioli, L. D., and Boman, H. G. (1982) Synthesis of the antibacterial peptide cecropin A (1−33), *Biochemistry 21*, 5020−5031.

37. Shai, Y., Bach, D., and Yanovsky, A. (1990) Channel formation properties of synthetic pardaxin and analogues, *J. Biol. Chem. 265*, 20202−20209.
38. Hackeng, T. M., Griffin, J. H., and Dawson, P. E. (1999) Protein synthesis by native chemical ligation: expanded scope by using straightforward methodology, *Proc. Natl. Acad. Sci. U.S.A. 96*, 10068−10073.
39. Boutonnet, N., Janssens, W., Boutton, C., Verschelde, J. L., Heyndrickx, L., Beirnaert, E., van der Groen, G., and Lasters, I. (2002) Comparison of predicted scaffold-compatible sequence variation in the triple-hairpin structure of human imunodeficiency virus type 1 gp41 with patient data, *J. Virol. 76*, 7595−7606.
40. Evans, T. C., Jr., Benner, J., and Xu, M. Q. (1998) Semisynthesis of cytotoxic proteins using a modified protein splicing element, *Protein Sci. 7*, 2256−2264.
41. Gazit, E., Miller, I. R., Biggin, P. C., Sansom, M. S., and Shai, Y. (1996) Structure and orientation of the mammalian antibacterial peptide cecropin P1 within phospholipid membranes, *J. Mol. Biol. 258*, 860−870.
42. Peisajovich, S. G., Epand, R. F., Pritsker, M., Shai, Y., and Epand, R. M. (2000) The polar region consecutive to the HIV fusion peptide participates in membrane fusion, *Biochemistry 39*, 1826−1833.
43. Kukol, A., Torres, J., and Arkin, I. T. (2002) A structure for the trimeric MHC class II-associated invariant chain transmembrane domain, *J. Mol. Biol. 320*, 1109−1117.
44. Jackson, M., and Mantsch, H. H. (1995) The use and misuse of FTIR spectroscopy in the determination of protein structure, *Crit. Rev. Biochem. Mol. Biol. 30*, 95−120.
45. Gazit, E., Lee, W. J., Brey, P. T., and Shai, Y. (1994) Mode of action of the antibacterial cecropin B2: a spectrofluorometric study, *Biochemistry 33*, 10681−10692.
46. Struck, D. K., Hoekstra, D., and Pagano, R. E. (1981) Use of resonance energy transfer to monitor membrane fusion, *Biochemistry 20*, 4093−4099.
47. Mozsolits, H., Wirth, H. J., Werkmeister, J., and Aguilar, M. I. (2001) Analysis of antimicrobial peptide interactions with hybrid bilayer membrane systems using surface plasmon resonance, *Biochim. Biophys. Acta 1512*, 64−76.
48. Papo, N., and Shai, Y. (2003) Exploring peptide membrane interaction using surface plasmon resonance: differentiation between pore formation versus membrane disruption by lytic peptides, *Biochemistry 42*, 458−466.
49. Sackett, K., and Shai, Y. (2003) How structure correlates to function for membrane associated HIV-1 gp41 constructs corresponding to the N-terminal half of the ectodomain, *J. Mol. Biol. 333*, 47−58.
50. Meng, F. G., Zeng, X., Hong, Y. K., and Zhou, H. M. (2001) Dissociation and unfolding of GCN4 leucine zipper in the presence of sodium dodecyl sulfate, *Biochimie 83*, 953−956.
51. Zhou, N. E., Kay, C. M., and Hodges, R. S. (1992) Synthetic model proteins. Positional effects of interchain hydrophobic interactions on stability of two-stranded alpha-helical coiled-coils, *J. Biol. Chem. 267*, 2664−2670.
52. Lau, S. Y., Taneja, A. K., and Hodges, R. S. (1984) Synthesis of a model protein of defined secondary and quaternary structure. Effect of chain length on the stabilization and formation of two-stranded alpha-helical coiled-coils, *J. Biol. Chem. 259*, 13253−13261.
53. Peisajovich, S. G., Samuel, O., and Shai, Y. (2000) Paramyxovirus F1 Protein Has Two Fusion Peptides: Implications for the Mechanism of Membrane Fusion, *J. Mol. Biol. 296*, 1353−1365.
54. Samuel, O., and Shai, Y. (2001) Participation of Two Fusion Peptides in Measles Virus-Induced Membrane Fusion: Emerging Similarity with Other Paramyxoviruses, *Biochemistry 40*, 1340−1349.
55. Kliger, Y., Peisajovich, S. G., Blumenthal, R., and Shai, Y. (2000) Membrane-induced Conformational Change During the Activation of HIV-1 gp41, *J. Mol. Biol. 301*, 905−914.
56. Heimburg, T., Schunemann, J., Weber, K., and Geisler, N. (1999) FTIR-Spectroscopy of multistranded coiled coil proteins, *Biochemistry 38*, 12727−12734.
57. Shnaper, S., Sackett, K., Gallo, S. A., Blumenthal, R., and Shai, Y. (2004) The C- and the N-terminal regions of glycoprotein 41 ectodomain fuse membranes enriched and not enriched with cholesterol, respectively, *J. Biol. Chem. 279*, 18526−18534.
58. Gallaher, W. R. (1987) Detection of a fusion peptide sequence in the transmembrane protein of human immunodeficiency virus, *Cell 50*, 327−328.
59. Rapaport, D., Ovadia, M., and Shai, Y. (1995) A synthetic peptide corresponding to a conserved heptad repeat domain is a potent inhibitor of Sendai virus-cell fusion: an emerging similarity with functional domains of other viruses, *EMBO J. 14*, 5524−5531.
60. Shugars, D. C., Wild, C. T., Greenwell, T. K., and Matthews, T. J. (1996) Biophysical characterization of recombinant proteins expressing the leucine zipper-like domain of the human immunodeficiency virus type 1 transmembrane protein gp41, *J. Virol. 70*, 2982−2991.
61. Bernstein, H. B., Tucker, S. P., Kar, S. R., McPherson, S. A., McPherson, D. T., Dubay, J. W., Lebowitz, J., Compans, R. W., and Hunter, E. (1995) Oligomerization of the hydrophobic heptad repeat of gp41, *J. Virol. 69*, 2745−2750.

BI047666G